Available free online at www.medjchem.com

*Mediterranean Journal of Chemistry* **2020**, 10(7), 697-707

# Modification of acid on beta zeolite catalysts by ion-exchange method for ethanol dehydration to diethyl ether

**Montri Thapplee, Chadaporn Krutpijit, Piyasan Praserthdam and Bunjerd Jongsomjit** *

Center of Excellence on Catalysis and Catalytic Reaction Engineering, Department of C Chemical Engineering,
Faculty of Engineering, Chulalongkorn University, Bangkok 10330, Thailand

**Abstract**: The catalytic ethanol dehydration to diethyl ether (DEE) over the synthesized beta zeolite (BEA) with different acidity on catalysts having Na and mixed Na-H forms was studied. The Na form of BEA catalyst was synthesized via the hydrothermal process, including non-calcined (Na-BEA_N) and calcined (Na-BEA_C) catalysts. The Na-BEA_C catalyst was successively used in the synthesis of different mixed Na-H forms under the ion-exchange method using the ammonium nitrate solution at 70°C for 2 h/cycle. In the present study, two different cycles were chosen, including one cycle (M-BEA_1) and four cycles (M-BEA_4) to compare the amount of acidity on catalysts. The results indicated that the M-BEA_1 catalyst exhibited a large surface area and contained the highest moderate acid site, which strongly affected the optimal catalytic activity at low temperature (<250°C) with ethanol conversion of 74.6% and DEE yield of 27.3%. However, the increased number of ion-exchange cycles had not shown remarkable effects on catalytic activity due to low surface area and moderate acidity.

**Keywords**: Beta zeolite; Diethyl ether; Ethanol dehydration; Ion-exchange.

## 1. Introduction

Currently, the increase of the population in the world consumes higher energy usage, such as nuclear, natural gas, coal, and fossil fuel oil [1]. Those energies are non-renewable, which are finite resources. Researchers are trying to find alternative energy for the replacement of natural fuels [2]. Renewable energy is becoming popular in research and development, including solar energy, hydropower energy, wind energy, and biomass energy [3]. Ethanol is a chemical compound produced via primary technology using the fermentation method of plants from renewable biomass resources such as corn, sugarcane, and cassava for the generation of liquid fuels. Usually, ethanol is mainly used as a biofuel additive by combination with petroleum distillates for transportation fuels such as gasoline and diesel engines. The outstanding feature of ethanol is the oxygenated chemical compound, which can reduce greenhouse gas emissions, e.g., $CO_2$, CO, and smoke in engines [4-7]. Nowadays, the production of ethanol becomes excess. Therefore, it is predicted that the excess ethanol will become available as a used raw material for the production of value-added chemical compounds shortly. Nevertheless, we can make the value-added of ethanol by selectively converting it into other chemical products such as diethyl ether, ethylene, acetaldehyde, butanol, acetic acid, etc. [8,9].

Diethyl ether (DEE) has the potential to open new pathways to produce petrochemicals from non-petroleum feedstock, which is an alternative source of clean, renewable energy. It is often widely used as a solvent in many industries, such as starting fluid for diesel and gasoline engines, general anesthetic during medical procedures, and solvent for pharmaceutical industries. Moreover, ethylene is one of the most important olefins, which is used as a major feedstock in the petrochemical industry to produce polyethylene, packaging materials, and PVC [10].

Ethanol can be converted to DEE and ethylene using the catalytic dehydration reaction. The formation of both products depends on the reaction temperature as the main factor. Ethylene is occurred via cracking of ethoxy group intermediate at high temperature with endothermic reaction. At the same time, DEE is generated at lower temperatures via an exothermic reaction, as shown in both reactions (1) and (2) [11-13].

$$C_2H_5OH \rightarrow C_2H_4 + H_2O \qquad \Delta H_{298} = +44.9 \text{ kJ/mol} \qquad (1)$$

$$2C_2H_5OH \rightarrow (C_2H_5)_2O + H_2O \Delta H_{298} = -25.1 \text{ kJ/mol} \qquad (2)$$

Many researchers have studied the relationship between catalyst properties and catalytic activity in ethanol dehydration. Commercial catalysts containing zeolite, including H-FER, H-MFI,

*Corresponding author: Bunjerd Jongsomjit*
*Email address: bunjerd.j@chula.ac.th*
DOI: http://dx.doi.org/10.13171/mjc107020081481bj

Received May 23, 2020
Accepted July 2, 2020
Published August 3, 2020

H-MOR, H-BEA, H-ZSM-5, H-Y, H-USY, and alumina were investigated [14-17]. Beta zeolite (BEA) is one type of zeolite catalysts having high silica zeolite, which is an attractive zeolite for a petrochemical reaction because it has porous structures, high thermal stability, high acidity, and large surface area. Also, the DEE and ethylene selectivities depend on the nature of the active site. As known, DEE formation is more favored for lower $SiO_2/Al_2O_3$ ratios, which correspond to a high acid density according to increased Al content in the zeolite framework [18,19]. The catalytic performance mainly depends on the acid sites available on the catalyst surfaces. The strong Brønsted acid sites play the primary duty for the conversion of ethanol to ethylene, while the moderate Bronsted acid sites are responsible for producing DEE [14,20]. An ion-exchange of $NH_4^+$ ions on the zeolite is used to obtain the mixed Na-H form in the zeolite structure, which is acidic catalysts [21]. Upon calcination of the ammonium zeolite, ammonia is driven off, leaving behind the acidic form of the zeolite. Then, protons reside at the ion exchange sites to generate an acid site of catalyst. The generation of the acid site can be described in 4 steps; i) the ammonium solution is added to create ammonium exchange by ion-exchange method, ii) $Na^+$ is exchanged by $NH_4^+$, iii) the $NH_3$ compound is decomposed by calcination to create an acid site ($H^+$ form), and iv) the $H^+$ form is in equilibrium, in which the silanol group is close to tricoordinate aluminium [22].

Many works of literature reported the catalytic ethanol dehydration over a variety of catalysts. However, beta zeolite has an attractive property in this reaction due to suitable acidity, acid strength, and physicochemical properties. Therefore, the synthesis of zeolite was chosen in this research to study the various factors that affect the performance of the catalyst. Besides, the modification of catalyst and the optimum ion-exchange cycle conditions to synthesis the modified beta zeolite has been addressed by a few approaches. Therefore, in the present study, our attention was focused on the catalyst properties of the synthesized beta zeolite catalysts prepared via the hydrothermal method followed by an ion-exchange process to obtain the catalysts with different Na and mixed Na-H forms. For the achievement of more detailed aspects, it may be useful to look more closely at the effect of catalytic preparation with different forms in zeolite catalysts to the gas-phase dehydration reaction of ethanol to DEE and ethylene.

## 2. Experimental

### 2.1. Materials

Tetraethylammoniumhydroxide solution (TEAOH) 40% in $H_2O$, silica nanopowder ($SiO_2$), and sodium aluminate ($NaAlO_2$) were purchased from Sigma-Aldrich Chemical Company, Inc. Sodium chloride (NaCl) and sodium hydroxide (NaOH) are Emsure® premium grade chemical products from Merck Company, Inc. Potassium chloride (KCl) was a product of Riedel-de Haën Company, Inc. Ammonium nitrate ($NH_4NO_3$) was obtained from Univar Company, Inc.

### 2.2. Catalyst preparation

Scheme 1 illustrates the synthesis strategy of BEA. The BEA catalysts were prepared via the hydrothermal method, following procedures described by M. A. Camblor [23].

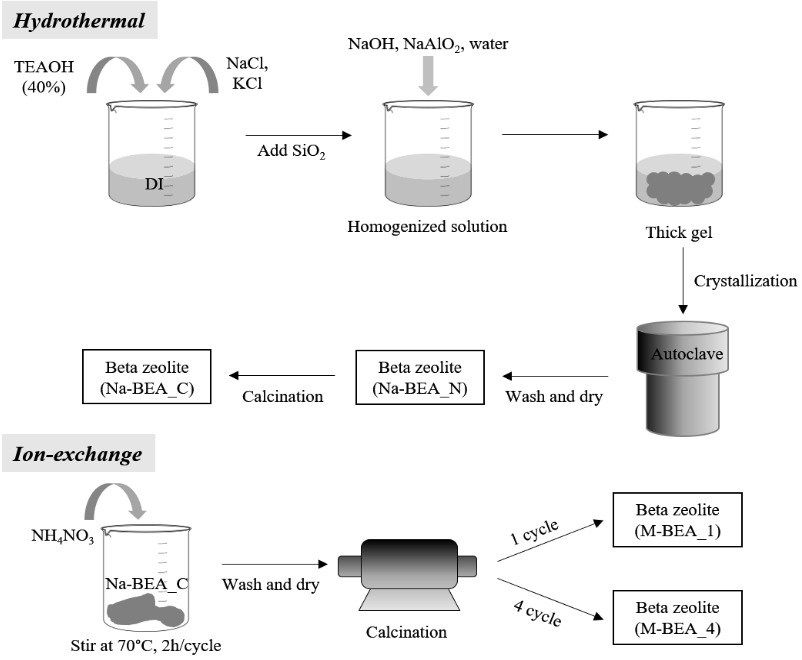

**Scheme 1.** Schematic diagram showing the synthesis of beta zeolite from the hydrothermal and ion-exchange method

In detail, 89.6 g of TEAOH was firstly mixed with NaCl (0.53 g), KCl (1.44 g) in 59.4 ml of deionized water, and 29.5 g of $SiO_2$ nanopowder was introduced sequentially. The solution was stirred until homogenized and then mixed with NaOH (0.33 g), $NaAlO_2$ (1.79 g), and 20 ml of water until obtaining a thick gel to get the Si/Al atomic ratio of 13. After that, it was transferred into a stainless-steel autoclave, and the zeolite was crystallized at 135°C for 20 h with agitation at 60 rpm. Finally, the obtained product was filtered and washed with deionized water until the obtained pH~9, and then dried at 110°C overnight. The non-calcined catalyst, which was defined as Na-BEA_N, was obtained. The Na-BEA_N was continuously calcined under airflow at 550°C for 6 h with a heating rate of 5°C/min. The calcined product was denoted as Na-BEA_C.

The different mixed Na-H forms were synthesized via the ion-exchange method using $NH_4NO_3$ (1 M) with the v/w ratio of 20 ml $NH_4NO_3/g_{cat}$ under continuous agitation at 70°C for 2 h/cycle. The various cycles, including one and four cycles of agitation, were studied. The obtained ion-exchange samples were washed with deionized water, filtered, and then dried at 110°C overnight. The collected samples were calcined under airflow at 550°C for 6 h to drive off the unstable components such as $NH_3$ and $NO_x$. The one and four cycles of the ion-exchange method were denoted as M-BEA_1 and M-BEA_4 catalysts, respectively.

## 2.3. Catalyst characterization

The crystalline phases of the catalysts were characterized using a SIEMENS D-5000 X-ray diffractometer with Cu $K_\alpha$ ($\lambda$ = 1.54439 Å). The spectra were scanned in the 2θ range of 10 to 50°. The surface area, average pore volume, and average pore diameter of the catalysts were analyzed by $N_2$ physisorption using a Micromeritics ASAP2000 automated system instrument. A Hitachi mode S-3400N was used to investigate the morphology of catalysts. Micrographs were taken at the accelerating voltage of 30 kV and magnification ranging from 1,000 to 10,000 and the resolution of 3 nm. The SEM was performed using the secondary scattering electron (SE) mode.

The elemental distribution mapping of catalysts was determined by using Link Isis series 300 program Energy-dispersive X-ray spectroscopy. The acidic properties of the catalysts were investigated using temperature-programmed desorption of ammonia ($NH_3$-TPD) using a micromeritics chemisorp 2750 pulse chemisorption system equipment. In order to perform the experiment, 0.05 g of catalyst was packed in a U-tube glass with 0.03 g of quartz wool and pretreated at 500°C under helium flow for 1 h. Then, the sample was saturated with 15% of $NH_3$/He and the physisorbed ammonia was desorbed under helium gas flow after saturation. The sample was heated from 40°C to 500°C at a heating rate of 10°C/min to desorb the chemisorbed $NH_3$.

## 2.4. Catalytic test

The gas-phase dehydration reaction of ethanol was performed in a fixed-bed continuous flow microreactor. In the experiment, 100 mg of catalyst was packed in the microreactor. Before the reaction, the catalyst sample was pretreated in a 60 ml/min flow rate of $N_2$ at 200°C for 1 h to remove some impurities from the catalyst surface. Then, the liquid ethanol was fed using a single-syringe pump at a constant flow rate of ethanol 1.45 ml/h into the reactor by vaporizing it under a flowing of $N_2$ at 120°C. The reaction temperature was carried out, ranging from 150 to 400°C. At each temperature, the reaction was carried out for ca. 1 h with 5 sample measurements. All chemicals in feed and product gas were detected and analyzed by a gas chromatograph with a capillary column (DB-5) connected to a flame ionization detector (FID).

# 3. Results and Discussion

## 3.1. Physicochemical properties

X-ray diffraction (XRD) technique was used to determine the characteristic phase and crystallinity of the BEA catalyst with different forms. The XRD patterns of BEA catalysts were recorded at 2θ values ranging from 10° to 50°. The XRD patterns (Figure 1) indicated the characteristic reflections of zeolite phase with a BEA type structure appearing at 2θ= 13.4°, 21.5°, 22.6°, 25.4°, 27.0° and 29.7° [23-25]. It may be expected that all catalysts were beta zeolite structure. The crystallinity of the samples correlated with dealumination. The crystallinity of the M-BEA_1 catalyst is higher than the Na-BEA_C catalyst corresponding to the lower Al content in the M-BEA_1 and the M-BEA_4 catalysts obtained from EDX measurement, as seen in Table 2. However, the diffraction peak of parent zeolite showed a low intensity in the M-BEA_4 catalysts. It might be presumed that the structure of catalyst might be destroyed form too much cycle of ion-change preparation.

The physical adsorption of $N_2$ gas was used as a probe molecule to analyze the specific surface area (BET surface area) and pore size diameter of the catalyst, as summarized in Table 1. The surface area of a Na form indicated that the Na-BEA_C catalyst was found to be higher than Na-BEA_N catalyst, while its pore size diameter was smaller. The reason is that the calcination process decomposes the organic template and generates the channels in the crystal structure of the catalyst. The mixed Na-H form showed that the surface area and pore size diameter of M-BEA_1 was much higher than that of M-BEA_4. This might be rationalized by the fact that the one cycle in the ion-exchange method could be decomposed ammonia species and rearranged Al structures from tetrahedral to octahedral via calcination of ammonium in zeolite structures resulting in increased surface area on M-BEA_1 catalyst [26].

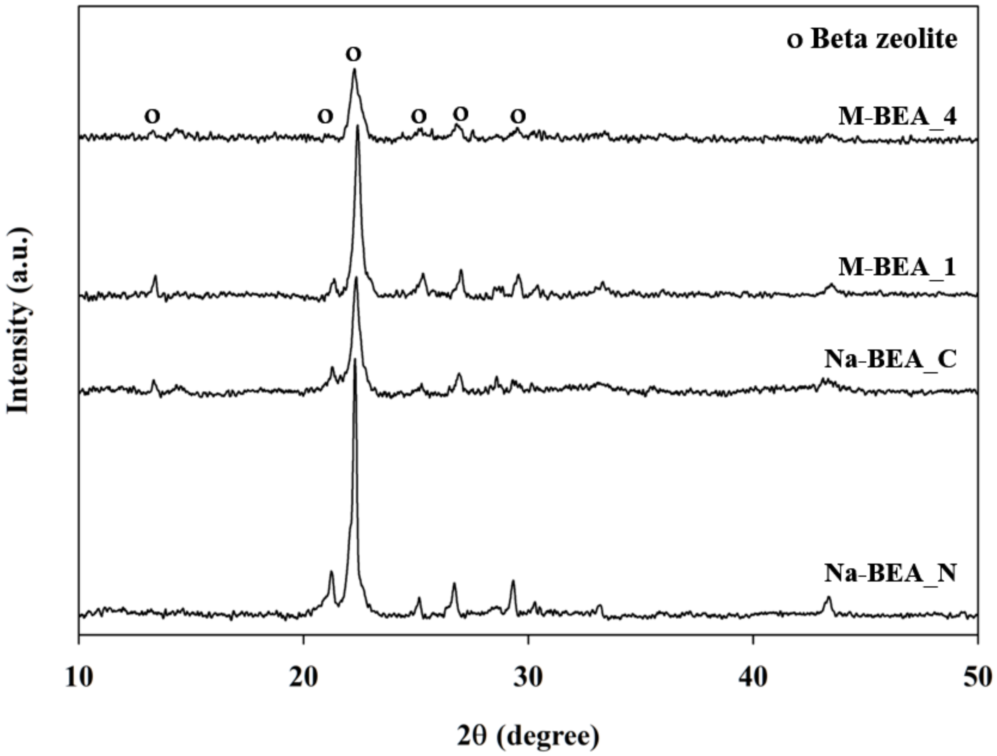

**Figure 1.** XRD patterns of the synthesized beta zeolite catalysts

In contrast, four cycles in the ion-exchange method led to the decomposition of Al atom, known as a dealumination reaction. This is likely due to the defect and partial collapse structures in zeolite that results in decreased surface area on the M-BEA_4 catalyst. A comparison between the Na and mixed Na-H form revealed that the mixed Na-H form (M-BEA_1) exhibited the highest surface area of 392.4 $m^2/g$, among other catalysts. As seen in Figure 2, the Na and mixed Na-H form catalysts represented the hysteresis loop between type I and IV curves, indicating the type of solid materials with micropores and mesopores material, according to the International Union of Pure and Applied Chemistry (IUPAC) classification [27].

**Table 1.** BET properties of the synthesized beta zeolite catalysts.

| Catalysts | BET surface area [a], $S_{BET}$ ($m^2/g$) | Pore size diameter [b] (nm) | Pore volume [b] ($cm^3/g$) |
|---|---|---|---|
| **Na-BEA_N** | 16 | 8.1 | 0.03 |
| **Na-BEA_C** | 236 | 5.4 | 0.04 |
| **M-BEA_1** | 392 | 4.4 | 0.05 |
| **M-BEA_4** | 196 | 4.1 | 0.03 |

[a] calculated from BET method

[b] calculated from BJH adsorption and desorption method

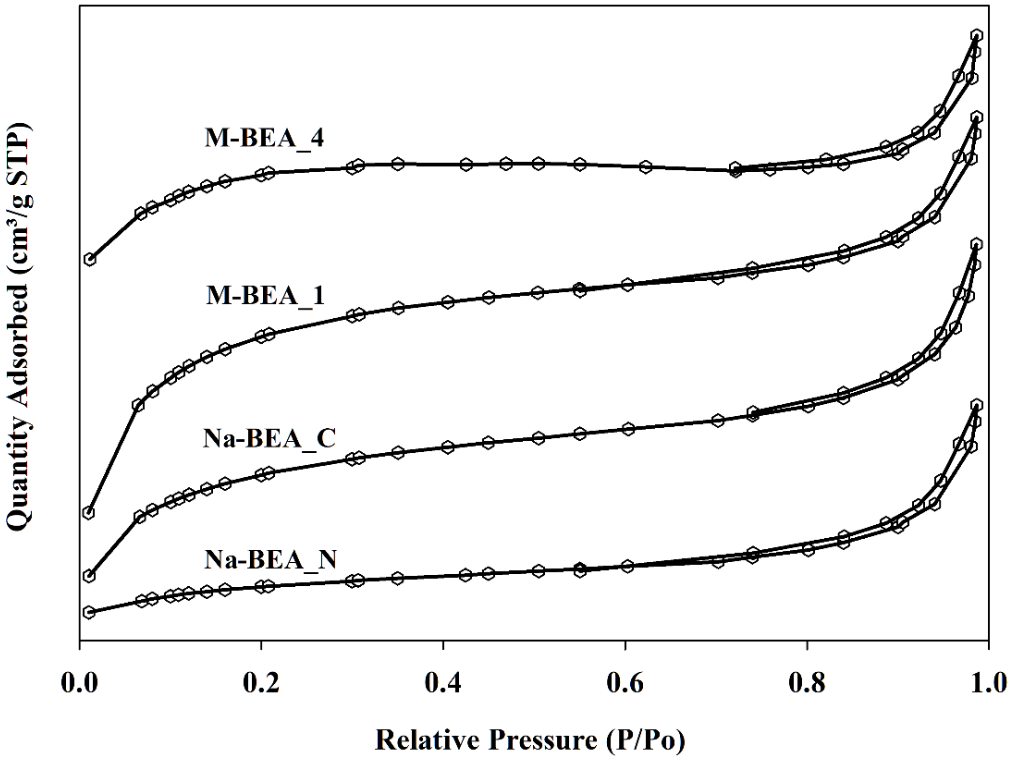

**Figure 2.** The $N_2$ adsorption-desorption isotherm of the synthesized beta zeolite catalysts

SEM technique was used to characterize the surface roughness of the material. The morphology on the surface of catalysts is shown in Figure 3. It was observed that the particle shapes of all catalysts are mostly spherical (round ball) and partially irregular [28]. The Na-BEA_N and Na-BEA_C represented the similar morphology in the round ball with some lumps formed. Nevertheless, the Na-BEA_C remained a little higher small lumps particle, which accompanied with the increase of surface area result. In the case of M-BEA_1 and M-BEA_4, it can be observed more top lumps formed, which can be attributed to the $H^+$ protonated zeolite and the $NH_4NO_3$ precursor of the catalyst. However, the different catalyst preparation methods did not affect the morphology of catalysts significantly. The quantity of elemental distribution on the catalyst surface was evaluated via the EDX spectroscopy, as summarized in Table 2. The result revealed that the Si/Al ratio increased with the number of calcinations. The Na-BEA_N catalyst exhibited the lowest Si/Al ratio of 5.9, while the Na-BEA_C was higher (6.1). For, the 2nd-calcined catalysts, the observed Si/Al ratios of M-BEA_1 and M-BEA_4 were 7.8 and 8.1, respectively, which was in a similar trend. The reason for this can be attributed to the dealumination after calcination. Additionally, the amount of Na elements drastically decreased about the ion-exchange method of catalyst preparation. It is presumably suggested that the BEA catalyst can exchange the ions between Na ions in the zeolite structures with ammonium ions in the ammonium nitrate solution during the ion-exchange process.

**Table 2.** Chemical composition obtained by EDX technique of the synthesized beta zeolite catalysts.

| Catalysts | Elemental distribution (wt%) | | | | |
|---|---|---|---|---|---|
| | Al | Si | O | Na | Si/Al |
| **Na-BEA_N** | 8.63 | 49.68 | 39.64 | 2.05 | 5.76 |
| **Na-BEA_C** | 8.84 | 51.97 | 37.38 | 1.82 | 5.88 |
| **M-BEA_1** | 6.98 | 50.89 | 41.65 | 0.48 | 7.29 |
| **M-BEA_4** | 6.84 | 51.53 | 41.85 | 0.29 | 7.53 |

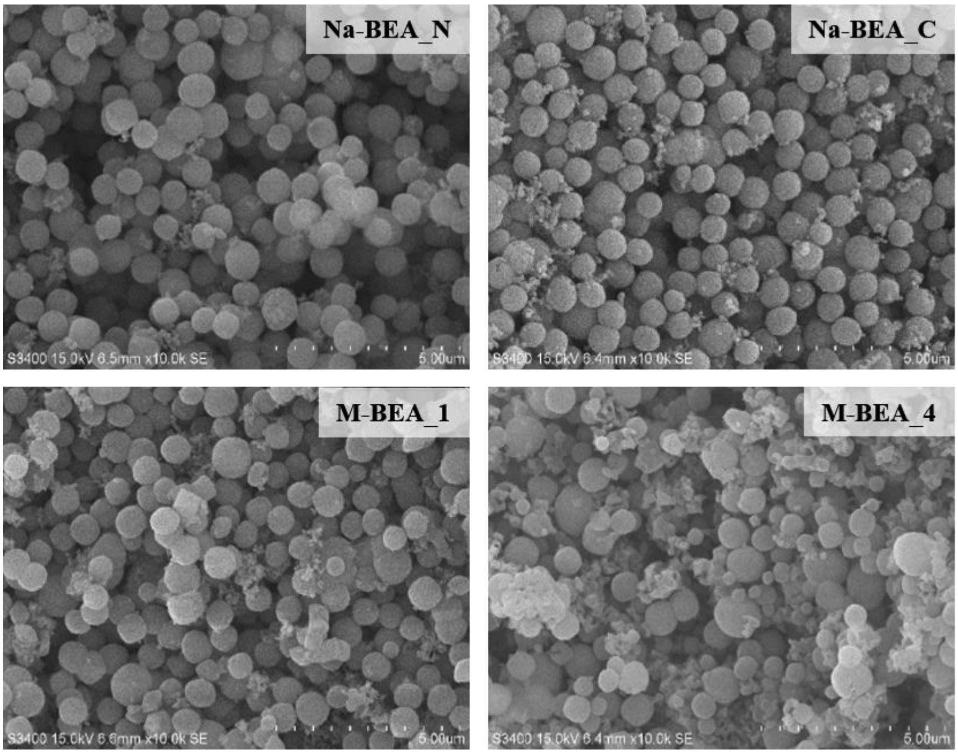

**Figure 3.** SEM images of the synthesized beta zeolite catalysts

To obtain a deeper insight into the acidity and acid strength properties of the catalyst that play important roles for the dehydration reaction, the $NH_3$-TPD measurement was performed. The ability of the active site in a catalytic dehydration reaction depends on the acidity and strength of the acid site. At higher temperatures, it exhibited a higher acid strength affecting the activity of the reactions. The $NH_3$-TPD technique can measure the acidity of the catalyst, but cannot divide the acid strength on the catalyst that is the limitation of this method [29]. However, the weak acid sites, in which the desorption peak appears at low temperatures below 250ºC, is possibly described as Lewis acid sites. In contrast, at higher temperatures, it is corresponding to Bronsted acid sites [30]. The $NH_3$-TPD profiles of catalysts having different forms are shown in Figure 4. The results demonstrated that all catalyst samples had three broad peaks located below 200°C, between 200-400°C and above 400°C due to the presence of the weak, moderate, and strong acid site, respectively. The number of acid sites with different strengths measured by the integration of ammonia desorption peak are listed in Table 3.

The results presented that the Na-BEA_N catalyst had the highest amount of total acid site (4,747.7 µmol $NH_3/g_{cat}$). However, it is not the amount of active site because this acidity is partially measured from acidic templates used in the synthesis of beta zeolite catalyst [31]. Nevertheless, the amount of total acid site of other catalysts tended to decrease as followed; Na-BEA_C (1,937.6 µmol $NH_3/g_{cat}$) > M-BEA_1 (1,888.0 µmol $NH_3/g_{cat}$) > M-BEA_4 (1,462.2 µmol $NH_3/g_{cat}$). These results are in good agreement with the observation of Chalupka et al. [32]. They reported that the calcined catalysts and ion-exchange methods reduce the amount of Al atom resulting in decreased total acidity in catalysts corresponding to the SEM-EDX technique, as shown in Table 2. When compared the acid strength on different forms of catalysts, it was observed that the highest weak, moderate, and strong acid sites were M-BEA_4, M-BEA_1, and Na-BEA_N catalysts, respectively. It is suggested that the ion-exchange method only affects the acid strength of catalysts.

**Table 3.** The acidic properties of the synthesized beta zeolite catalysts determined by temperature-programmed desorption of $NH_3$.

| **Catalysts** | **Number of acid site (µmol $NH_3/g_{cat}$)** | | | |
|---|---|---|---|---|
| | **Weak** | **Moderate** | **Strong** | **Total** |
| **Na-BEA_C** | 226.8 | 1,193.8 | 516.9 | 1,937.6 |
| **M-BEA_1** | 135.7 | 1,232.6 | 519.7 | 1,888.0 |
| **M-BEA_4** | 519.6 | 405.7 | 536.9 | 1,462.2 |

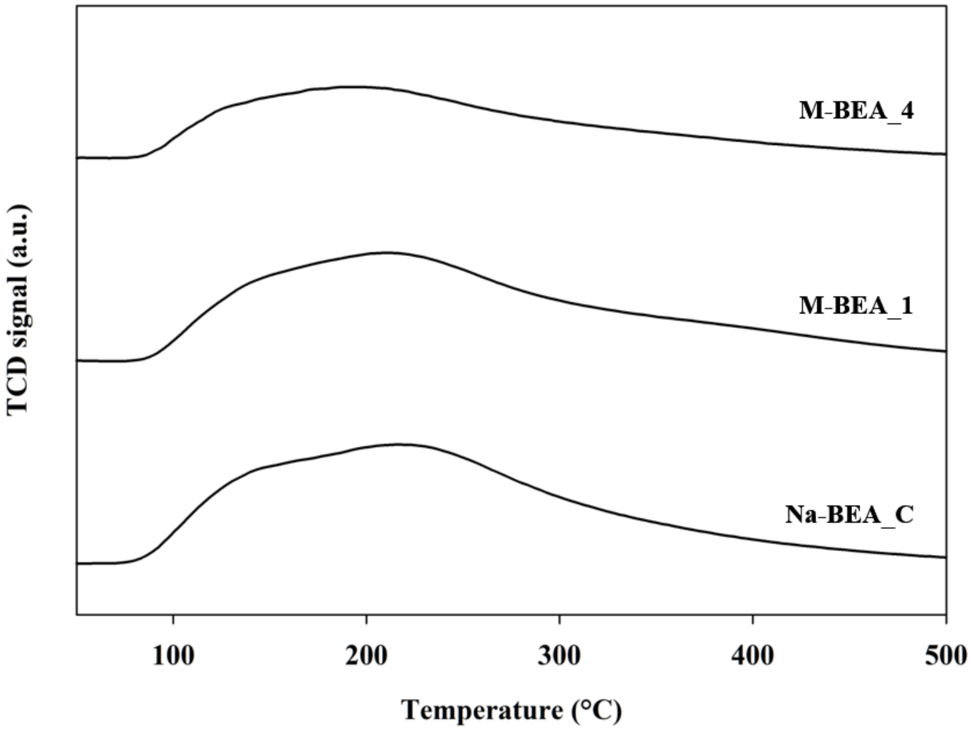

**Figure 4.** $NH_3$-TPD profiles of the synthesized beta zeolite catalysts

### 3.2. Catalytic performance

Vapor phase ethanol dehydration over prepared BEA catalysts, including Na-BEA_N, Na-BEA_C, M-BEA_1, and M-BEA_4, was performed to evaluate the catalytic activity, the ethanol conversion, selectivity and yield of products such as DEE, ethylene, and acetaldehyde at various temperatures. The reaction temperatures in this study ranged from 150°C to 400°C under atmospheric pressure. The results of ethanol conversion upon different reaction temperatures are displayed in Figure 5.

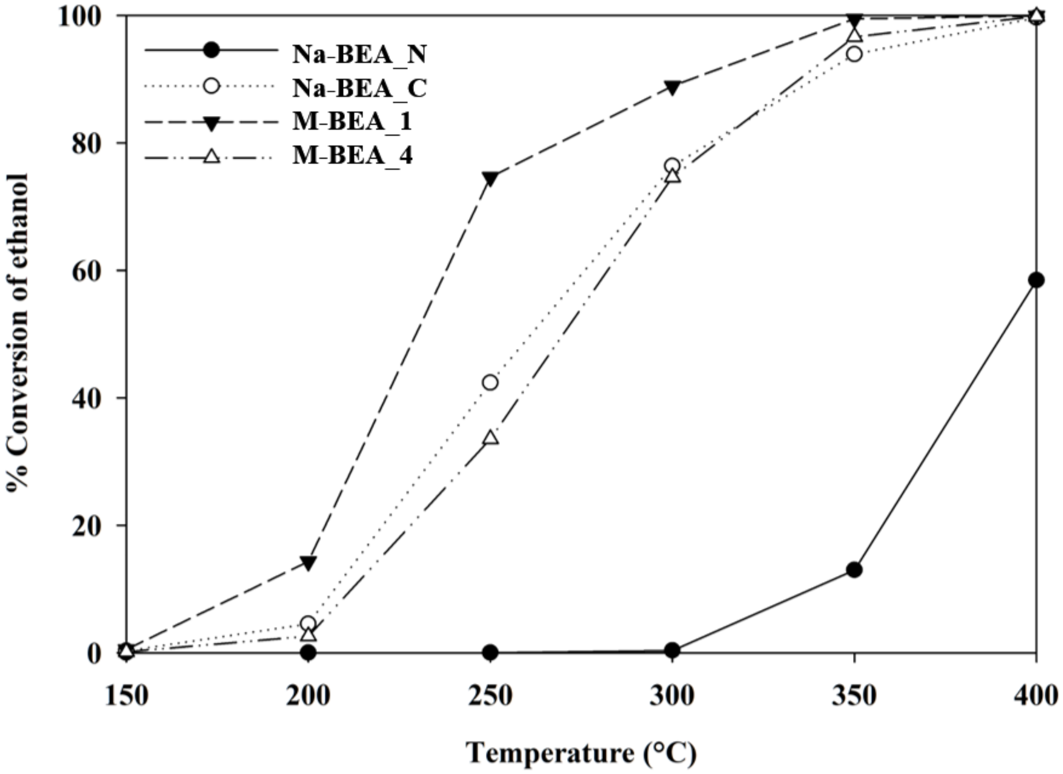

**Figure 5.** Ethanol conversion of the synthesized beta zeolite catalysts

Notably, the conversion of ethanol increases with increasing reaction temperature, which gives a rise in the equilibrium constant (K), resulting in a shift of reactant to the products [33]. As expected, all catalysts in this study exhibited an increase in ethanol conversion by increasing the temperature. It can be seen that the mixed Na-H form (M-BEA_1) showed the highest ethanol conversion for all reaction temperatures, whereas the Na-BEA_N exhibited the lowest conversion of ethanol. This result mainly came from the absence of calcination in Na-BEA_N because this catalyst did not decompose the organic template and generate the channels in the crystals.

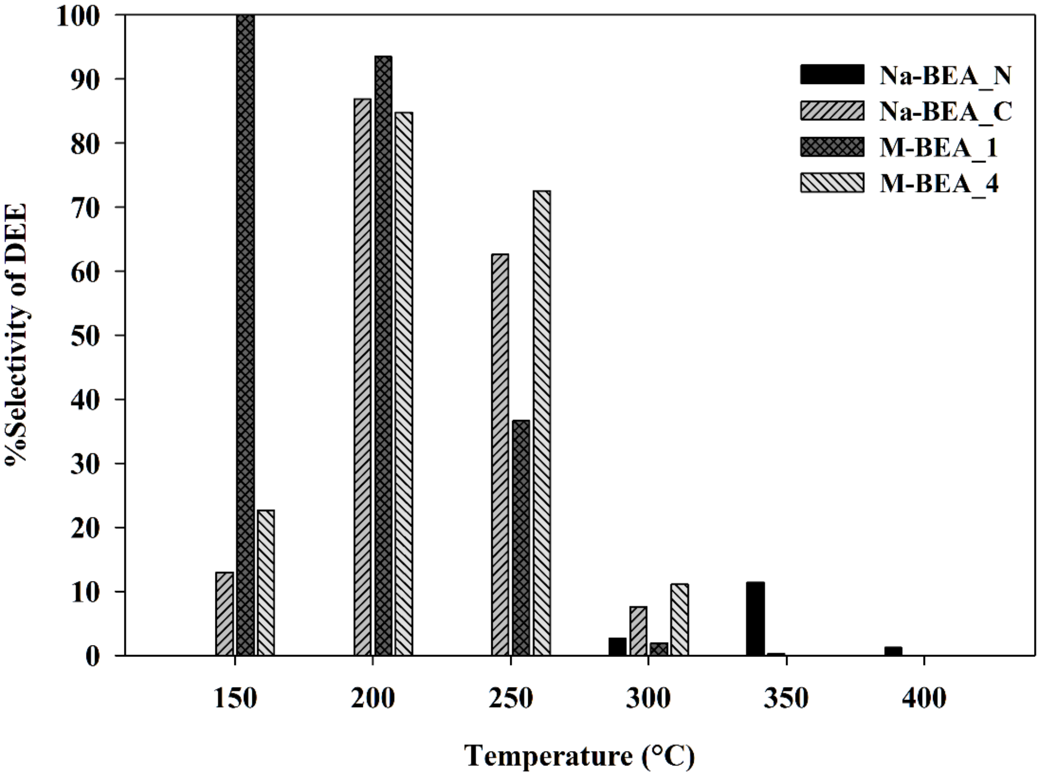

**Figure 6.** DEE selectivity of the synthesized beta zeolite catalysts

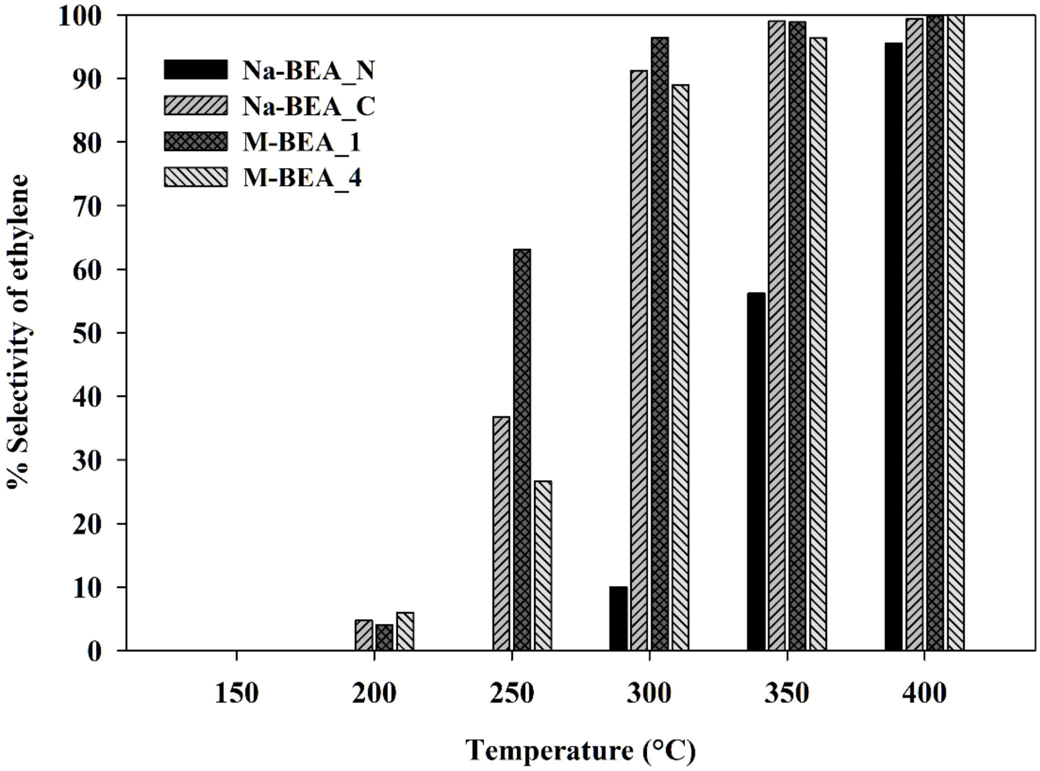

**Figure 7.** Ethylene selectivity of the synthesized beta zeolite catalysts

**Table 4**. All product yields of the synthesized beta zeolite catalysts.

| Catalysts | Temperature (°C) | Product yield (%) | | |
|---|---|---|---|---|
| | | DEE | Ethylene | Acetaldehyde |
| **Na-BEA_N** | 150 | 0.0 | 0.0 | 0.0 |
| | 200 | 0.0 | 0.0 | 0.0 |
| | 250 | 0.0 | 0.0 | 0.0 |
| | 300 | 0.0 | 0.0 | 0.3 |
| | 350 | 1.5 | 7.3 | 4.2 |
| | 400 | 0.7 | 55.8 | 1.9 |
| **Na-BEA_C** | 150 | 0.0 | 0.0 | 0.2 |
| | 200 | 3.9 | 0.2 | 0.4 |
| | 250 | 26.5 | 15.6 | 0.3 |
| | 300 | 5.8 | 69.6 | 0.9 |
| | 350 | 0.2 | 92.9 | 0.8 |
| | 400 | 0.0 | 98.9 | 0.7 |
| **M-BEA_1** | 150 | 0.5 | 0.0 | 0.0 |
| | 200 | 13.4 | 0.6 | 0.4 |
| | 250 | 27.3 | 47.0 | 0.3 |
| | 300 | 1.7 | 85.7 | 1.5 |
| | 350 | 0.0 | 98.3 | 1.1 |
| | 400 | 0.0 | 99.7 | 0.2 |
| **M-BEA_4** | 150 | 0.0 | 0.0 | 0.1 |
| | 200 | 2.2 | 0.2 | 0.2 |
| | 250 | 24.3 | 8.9 | 0.3 |
| | 300 | 8.3 | 66.3 | 0.0 |
| | 350 | 0.1 | 93.1 | 3.5 |
| | 400 | 0.0 | 99.8 | 0.0 |

The selectivities to DEE and ethylene for the dehydration reaction are presented in Figures 6 and 7, respectively, indicating that the main products are DEE and ethylene. The results demonstrated that the selectivity of DEE decreased with increasing the temperature, whereas the ethylene selectivity was contrary. It can be seen that the M-BEA_1 catalyst can achieve the complete DEE selectivity at 150°C. The product yields of different forms in catalysts are listed in Table 4. It can be noticed that the DEE yield increased when the reaction temperature reached 250°C and dramatically decreased when the reaction temperature was raised. The obtained DEE yields were ranged between 0-27.3% at 250°C. The dehydration activity decreased in the following order: M-BEA_1 > Na-BEA_C > M-BEA_4 > Na-BEA_N. The obtained highest DEE yield of M-BEA_1 was following the largest surface area and the amount of moderate acid site (329.4 $m^2/g$, 1,232.6 $\mu mol\ NH_3/g_{cat}$), while the lowest DEE yield of Na-BEA_N was corresponding to the least surface area and the amount of moderate acid site (15.8 $m^2/g$, 70.4 $\mu mol\ NH_3/g_{cat}$). Interestingly, the dehydration activity of M-BEA_4 was found to be lower than M-BEA_1 because the surface area and the number of moderate acid sites were relatively lower. This finding suggests that increasing the number of ion-exchange cycles caused a decrease in the surface area and the amount of modest acid site, consequently leading to a reduction in dehydration activity. One can verify that DEE selectivity is dominant at the temperature below 250°C. On the contrary, ethylene is a primary product at high temperatures (above 250°C). It is generally accepted that ethanol conversion can undergo via acid-base catalyzed reaction. Therefore, acetaldehyde is also found as a byproduct formed by the dehydrogenation reaction.

## 4. Conclusion

The synthesized beta zeolite catalysts with different forms, including Na and mixed Na-H form, were characterized and investigated upon the catalytic performance in the ethanol dehydration reaction. The XRD and $N_2$ physisorption results confirmed that the synthesized catalyst is “beta zeolite”. The finding demonstrated that the preparation of the catalyst by the ion-exchange method improved the moderate acid site of the catalyst, which can play an essential role in primary alcohol dehydration. It can be concluded that the mixed Na-H form (M-BEA_1) catalyst with one cycle in the ion-exchange method (M-BEA_1) is a suitable catalyst to convert ethanol to DEE because it exhibited the optimal catalytic activity at low temperature (250°C) with ethanol conversion of 74.6% and DEE yield of 27.3%. The reason is that this catalyst has the highest surface area resulting in increased accessibility for the number of adsorbed ethanol reactants and the proper amount of moderate acid site that is selective to DEE formation at low temperatures.

## Acknowledgments

This research is funded by Chulalongkorn University and Cat-Reac industrial project.

## References

1- M. M. Balmaceda, Differentiation, materiality, and power: Towards a political economy of fossil fuels, Energy Research & Social Science, **2018**, 39, 130-140.

2- J. A. Bolanos, Energy, uncertainty, and entrepreneurship: John D Rockefeller's sequential approach to transaction costs management in the early oil industry, Energy Research & Social Science, **2019**, 55, 26-34.

3- J. A. McGee, P. T. Greiner, Renewable energy injustice: The socio-environmental implications of renewable energy consumption, Energy Research & Social Science, **2019**, 56, 101214.

4- S. Rahmani, M. Rezaei, F. Meshkani, Preparation of highly active nickel catalysts supported on mesoporous nanocrystalline $\gamma\text{-A}_{l2}\text{O}_3$ for $CO_2$ methanation, Journal of Industrial and Engineering Chemistry, **2014**, 20, 1346-1352.

5- F. Ocampo, B. Louis, A.-C. Roger, Methanation of carbon dioxide over nickel-based $Ce_{0.72}Zr_{0.28}O_2$ mixed oxide catalysts prepared by sol-gel method, Applied Catalysis A: General, **2009**, 369, 90-96.

6- J. W. Akitt, Some observations on the greenhouse effect at the Earth's surface, Spectrochimica Acta Part A: Molecular and Biomolecular Spectroscopy, **2018**, 188, 127-134.

7- T. R. Anderson, E. Hawkins, P. D. Jones, $CO_2$, the greenhouse effect and global warming: from the pioneering work of Arrhenius and Callendar to today's Earth System Models, Endeavour, **2016**, 40, 178-187.

8- J. Sun, Y. Wang, Recent Advances in Catalytic Conversion of Ethanol to Chemicals, ACS Catalysis, **2014**, 4, 1078-1090.

9- G. W. Huber, S. Iborra, A. Corma, Synthesis of Transportation Fuels from Biomass: Chemistry, Catalysts, and Engineering, Chemical Reviews, **2006**, 106, 4044-4098.

10- J. Janlamool, B. Jongsomjit, Catalytic Ethanol Dehydration to Ethylene over Nanocrystalline $\chi$- and $\gamma\text{-Al}_2\text{O}_3$ Catalysts, Journal of Oleo Science, **2017**, 66, 1029-1039.

11- J. C. Soh, S. L. Chong, S. S. Hossain, C. K. Cheng, Catalytic ethylene production from ethanol dehydration over non-modified and phosphoric acid modified Zeolite H-Y (80) catalysts, Fuel Processing Technology, **2017**, 158, 85-95.

12- G. Chen, S. Li, F. Jiao, Q. Yuan, Catalytic dehydration of bioethanol to ethylene over $TiO_2/\gamma\text{-}Al_2O_3$ catalysts in microchannel reactors, Catalysis Today, **2007**, 125, 111-119.

13- Y. Chen, Y. Wu, L.Tao, B. Dai, M. Yang, Z. Chen, X. Zhu, Dehydration reaction of bio-ethanol to ethylene over modified SAPO catalysts, Journal of Industrial and Engineering Chemistry, **2010**, 16, 717-722.

14- T. K. Phung, L. Proietti Hernández, A. Lagazzo, G. Busca, Dehydration of ethanol over zeolites, silica alumina and alumina: Lewis acidity, Brønsted acidity, and confinement effects, Applied Catalysis A: General, **2015**, 493, 77-89.

15- T. K. Phung, G. Busca, Ethanol dehydration on silica-aluminas: Active sites and ethylene/diethyl ether selectivities, Catalysis Communications, **2015**, 68, 110-115.

16- T. K. R. de Oliveira, M. Rosset, O. W. Perez-Lopez, Ethanol dehydration to diethyl ether over Cu-Fe/ZSM-5 catalysts, Catalysis Communications, **2018**, 104, 32-36.

17- D. Zhang, R. Wang, X. Yang, Effect of P Content on the Catalytic Performance of P-modified HZSM-5 Catalysts in Dehydration of Ethanol to Ethylene, Catalysis Letters, **2008**, 124, 3, 384-391.

18- W. Choopun, S. Jitkarnka, Catalytic activity, and stability of HZSM-5 zeolite and hierarchical uniform mesoporous MSU-$S_{ZSM}$-5 during bio-ethanol dehydration, Journal of Cleaner Production, **2016**, 368-378.

19- C. Yen Wu, H. Shing Wu, Ethylene Formation from Ethanol Dehydration Using ZSM-5 Catalyst, ACS Omega, **2017**, 2, 4287-4296

20- A. E.-A. A. Said, M. M. M. Abd El-Wahab, M. M. Abdelhak, The role of Brønsted acid site strength on the catalytic performance of phosphotungstic acid supported on nano $\gamma$-alumina catalysts for the dehydration of ethanol to diethyl ether, Reaction Kinetics, Mechanisms and Catalysis, **2017**, 122, 433-449.

21- H. G. Karge, Post-synthesis modification of microporous materials by solid-state reactions, Surface Science and Catalysis, Elsevier, **1997**, 105, 1901-1948.

22- R. P. Townsend, E. N. Coker, Chapter 11 Ion exchange in zeolites, Studies in Surface Science and Catalysis, Elsevier, **2001**, 137, 467-524.

23- M. A. Camblor, J. Perez-Pariente, Chapter 31-BEA Zeolite Beta Si(93), Al(7), Verified

Syntheses of Zeolitic Materials, Elsevier, **2001**, 115-117.

24- T. Kamsuwan, P. Praserthdam, B. Jongsomjit, Diethyl Ether Production during Catalytic Dehydration of Ethanol over Ru- and Pt-modified H-beta Zeolite Catalysts, Journal of Oleo Science, **2017**, 66, 199-207.

25- G. Ye, Y. Sun, Z. Guo, K. Zhu, H. Liu, X. Zhou, M.O. Coppens, Effects of zeolite particle size and internal grain boundaries on Pt/Beta catalyzed isomerization of n-pentane, Journal of Catalysis, **2018**, 360, 152-159.

26- A. Vimont, F. Thibault-Starzyk, J. C. Lavalley, Infrared Spectroscopic Study of the Acidobasic Properties of Beta Zeolite, The Journal of Physical Chemistry B, **2000**, 104, 286-291.

27- S. T. F. Grecco, E. A, Urquieta-González, P. Reyes, M. Oportus, M. d. C. Rangel, Influence of Temperature and Time of Seed Aging on the Properties of Beta Zeolite/MCM-41 Materials, Chem. Soc., **2014**, 25, 2444-2454.

28- A. Sher, Characterization of Beta Zeolites by X-Ray Diffraction, Scanning Electron Microscope, and Refractive Index Techniques, J. Chem. Soc. Pak., **2010**, 32, 592-598.

29- F. Lónyi, J. Valyon, On the interpretation of the $NH_3$-TPD patterns of H-ZSM-5 and H-mordenite, Microporous and Mesoporous Materials, **2001**, 47, 2, 293-301.

30- L. Martins, D. Cardoso, P. Hammer, T. Garetto, S. H. Pulcinelli, C. V. Santilli, Efficiency of ethanol conversion induced by controlled modification of pore structure and acidic properties of alumina catalysts, Applied Catalysis A: General, **2011**, 398, 59-65.

31- J. Weitkamp, Zeolites and catalysis, Solid State Ionics, **2000**, 131, 175-188.

32- K. Chalupka, R. Sadek, L. Valentin, Y. Millot, C. Calers, M. Nowosielska, J. Rynkowski, S. Dzwigaj, Dealuminated Beta Zeolite Modified by Alkaline Earth Metals, Journal of Chemistry, **2018**, 2018, 1-11.

33- A. Lima, A. J De Assis, C. Hori, M. Reis, A. E. Da Hora Machado, Thermodynamic Analysis of Ethanol Dehydration to Ethylene through Equilibrium Constant Method Using Classic Thermodynamics and Quantum Chemistry, International Review of Chemical Engineering, **2012**, 4, 466-473.